C-Band Monopulse Planar Array and Feeding Network

Marcelo B. Perotoni[1] ⓘ, Sergio Tavares[2] ⓘ, Bruno C. de S. Sanches[2] ⓘ, Walter J. Silva [1] ⓘ
Sergio T. Kofuji[2] ⓘ

[1]CECS-UFABC, Brazil, marcelo.perotoni@ufabc.edu.br and prof.walterjs@gmail.com,
[2]LSI-EPUSP, Brazil, tavares.st@pad.lsi.usp.br, bruno.ctt@gmail.com and kofuji@usp.br

Abstract— **Monopulse radars operate with simultaneous beams and are used for tracking purposes, relying only on hardware to provide a real-time indication of the target position. A monopulse array and its feeding network is implemented and tested, in the frequency of 5.4 GHz, based on patch antennas using dieletric to provide wide bandwidth and high gain. The system field styrofoam as pattern was evaluated in two different environments, a shielded room and an indoor area. Results agreed with simulation for either individual elements as well as the final integrated monopulse array.**

Index Terms— C-band, monopulse radar, radar, tracking.

I. INTRODUCTION

A monopulse radar generates spatially orthogonal beams for purposes of scanning and tracking targets. They were devised to replace onboard, mechanically rotated antennas [1], which sometimes turned out to be cumbersome and difficult to fit into aircraft tight spaces. Tough initially suffering from complex circuitry due to their waveguide technology, off-the-shelf circuitry enabled onboard monopulse radars to be operated even in missiles [2], where space is scarce. Found in operation even in lower frequencies for Early Warning Systems (245 MHz) [3] they usually benefit from the size reduction and improved resolution obtained in case of smaller wavelenghts, such as X-Band [4], where ingenuous waveguide arrangements provide high-gain using horns [5] and reflectors [6] at expenses of refined and complex mechanical construction. An L-band planar monopulse was designed to be placed in an external pod on top of an airplane, with 18-elements, covering the range of 1.02 to 1.1 GHz [7]. Benefiting from a SIW (substrate-integrated waveguide) technology, an X-band integrated monopulse was designed and tested, using a substrate with dielectric constant of 2.4 and operating with a slot antenna array [8]. Monopulses are also utilized for educational purposes while teaching radar and antenna array subjects, examples such as using commercial WiFi antennas and Matlab for processing [9] or commercial horn antennas coupled to a planar hybrid, operating at 2 GHz [10]. Target tracking can be observed without the need of non-real time processing, so it enables a clear and straightforward understanding of complex issues related to antennas and beamforming arrays in classroom.

The simultaneous beams are usually based on an antenna array fed by a 180° hybrid, the basic idea

depicted in Fig. 1. The orthogonal beams are created in real-time and at the same time, with their individual detected RF energies available in the Sum (or Sigma) and Difference (or Delta) ports. In contrast to baseband-processing relying on DSPs or other digital processing coming after analog-to-digital conversion, information on the target position is available by monitoring signals on the 180° hybrid (rat-race in the planar version or magic-T in waveguide) terminals. In the simplest case, a plain amplitude measurement of either ports gives a rough idea of the position, in the plane containing the array, as exemplified in the two colored targets in Fig. 1 and their respective amplitude levels in both ports. Besides amplitude monopulses, there can be also phase monopulses, though modern versions combine both, the so-called hybrid receivers [11]. Further processing can expand the information present in the sigma and delta ports, after digitized the tracking performance can be improved with functions such as anti-jamming, pulse compression and compensation for hardware phase errors [12]. Cross-correlation, in particular, was shown to improve the target identification in cases of multiple echos due to other reflectors, when wide band signals are used in the array [13].
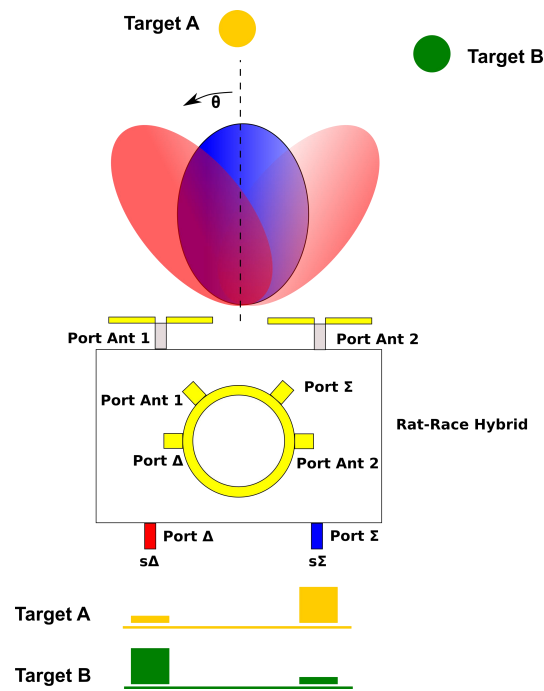

Fig. 1. Block diagram of the monopulse system, based on a planar 180° hybrid. The different colors red and blue illustrate the simultaneous beams at both ports. Two fictitious targets (yellow and green), in two angular positions generate different amplitudes in the ports, shown at the bottom part.

The hybrid-fed array generates two simultaneous beams, one where the antennas are in-phase (maximum radiaton at boresight) and the other with the elements anti-phase fed (180°), with the minimum in this same direction. In the example, it therefore implements a simple two-antenna array, whose weights can be written as [1,1] for the sum port and [1,-1] for the difference port, ideally. The antenna elements define the subsequent farfield pattern which is spatially multiplied by the array factor, defined by the aforementioned weights and the inter-element distance. For the sake of

performance, high-gain antennas (pencil-beam) offer the advantage of lower sensitivity to clutter and undesired reflections that are absorbed by the side and back-lobes, thereby increasing the minimum detected signal-to-ratio.

This article describes a planar monopulse system operating at 5.4 GHz (C Band). This band was chosen to comply with existing weather and surveillance systems and also because the prototyping is still possible with the available resources. Laboratory instrumentation also imposed an upper frequency limit, particularly within the anechoic chamber. It employs patch antennas with air as dielectric, as a way to increase the bandwidth and also their gains, while keeping the fabrication costs low. The antenna lower Q also relaxes the sensitivity to fabrication errors, easing the prototyping when sophisticated machining resources are not available. The integrated monopulse is tested in two different environments, after individual elements are analyzed and presented. It is intended to be used as antennas and RF laboratory example, demonstrating applied electromagnetics concepts and integrated microwave and RF instrumentation.

II.   ANTENNA AND HYBRID DESIGNS

Patch antennas were selected due to their robustness and their uncomplicated manufacturing with common available tools, resulting in moderate gain levels and lower backside radiation. Among the techniques to improve their inherently narrow bandwidth, lowering the overall structure Q [14], air was selected to be used as dielectric due to its low dielectric constant, both real (unitary) and imaginary (close to zero), the latter proportional to losses. Another alternative to increase the bandwidth of patch antennas in reported monopulse applications involved the use of proximity coupling, at expenses of a more complex design [15], which resulted in 28.2 % impedance bandwidth for VSWR≤2. Using a non-planar approach, a monopole-based monopulse covered the UWB range, 5.5 to 9 GHz, with the inclusion of a reflector backing the radiating elements [16]. The used antennas here employed 4-mm thick Styrofoam as spacing between the radiating elements and the ground plane, considering that this material has very similar properties to the air. The elements were set to be square and optimized using FEKO Method of Moments, which is particularly adequate to pure metallic structures. The patches were manually cut out from a 0.02 mm thick copper sheet, with a scissor. The ground planes, which used a thicker metallic sheet, were cut with a sheet-cutting scissor. Table I contains the comparison of the two prototyped antennas with the simulation. In spite of the manual construction the results show a good correlation, with measured bandwidths close to 10%. Effects of non-ideal SMA connectors and their associated vertical transition were not included in the virtual model, which was modeled inside FEKO as a simple 50 Ω wire port. The antennas were measured isolated, not in the array, so mutual coupling effects that arise later were not taken into account. Fig. 2 contains the picture of the elements, their dimensions and the S11 response, both simulated and measured.

TABLE I − COMPARISON OF THE TWO CONSTRUCTED ANTENNAS AGAINST THE SIMULATION.

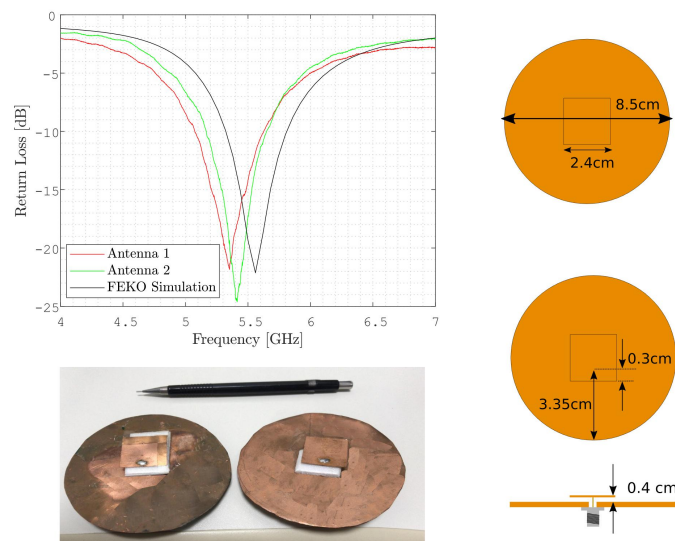|	Resonant frequency [GHz]	10-dB Bandwidth [GHz]	Relative Bandwidth [%]	% offset compared to simulation
Ant. #1	5.41	5.08-5.63	10.16	2.69
Ant. #2	5.35	5.17-5.65	8.97	3.77
Simulated	5.56	5.32-581	8.82	-

Fig. 2. Comparison of the two antennas (bottom) against the FEKO simulation (top). Dimensions of the individual elements are shown at the right, including the feed placement.

Regarding the antenna element farfield pattern, within the 5.32 to 5.81 GHz range, the maximum simulated gain is on average 10.55 dB, according to Fig. 3. A 3D plot is shown to illustrate the orientation of the main lobe and the back-side radiation, for the particular frequency of 5.4 GHz. The front-to-back radiation relation at this same frequency was simulated to be 16.7 dB, which is important for radar and tracking purposes since radiation from other directions does not add to the reflected signal from the target.

A measurement was performed in an open area for the angular range of 180° around the boresight, Fig. 4 shows the results for the normalized received power for a single element. It can be seen that the simulation agrees to the measurement particularly close to the main beam. Deviations can be accounted to the reflections caused by the non-ideal environment, discussed in the next section and shown in Fig. 10.
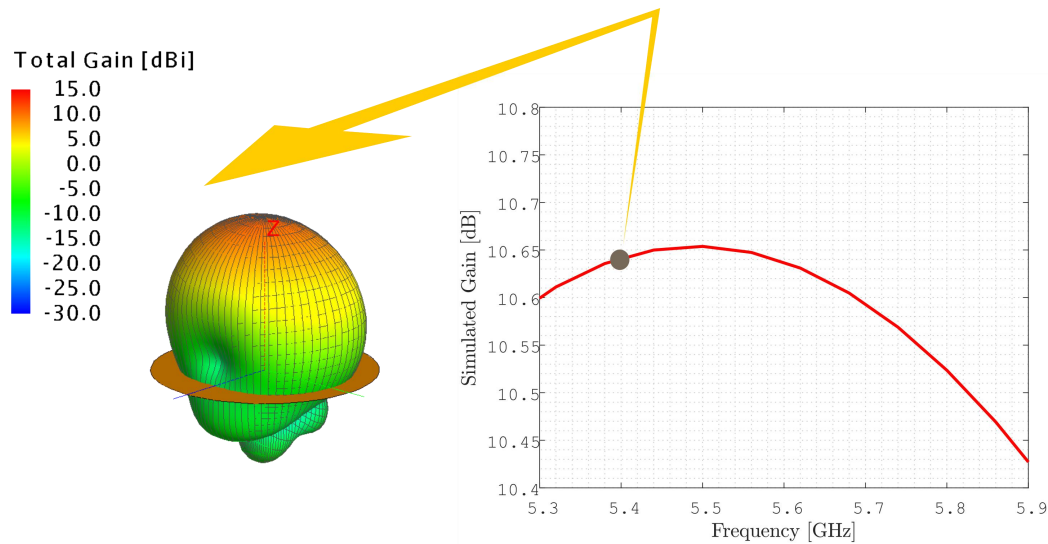
411

Fig. 3. (Right) simulated gain variation over the antenna in the -10 dB S11 frequency range. (Left) simulated 3D plot of the gain at the frequency of 5.4 GHz, shown overlapped with the antenna.
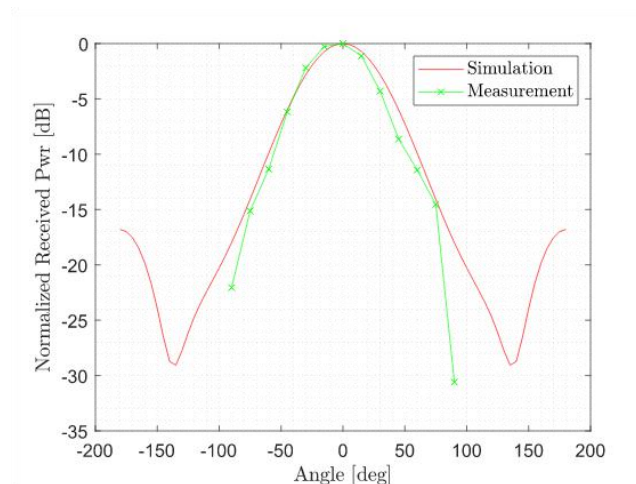

Fig. 4. Comparison of the single element farfield power pattern, normalized, at the frequency of 5.4 GHz.

The 180° hybrid, or rat-race, was designed following standard rules [18] and prototyped using a drilling machine, on a 0.508 mm thick Arlon substrate, and it is presented alongside the measured ports return loss in Fig. 5. All four ports insertion losses are below -10 dB in the range of 4.96 to 5.58 GHz. Its phase error for both sigma/sum and delta/difference ports is smaller than 11°, where the sigma has to be ideally 0° and delta 180°. The amplitude error in the aforementioned range is smaller than 0.8 dB, where it ideally should be 3 dB for either ports. Fig. 6 contains the amplitude and phase error plots.

Considering the combined antennas and hybrid overlapped responses, the bandwidth of the system can be estimated to extend from 5.17 to 5.58 GHz.
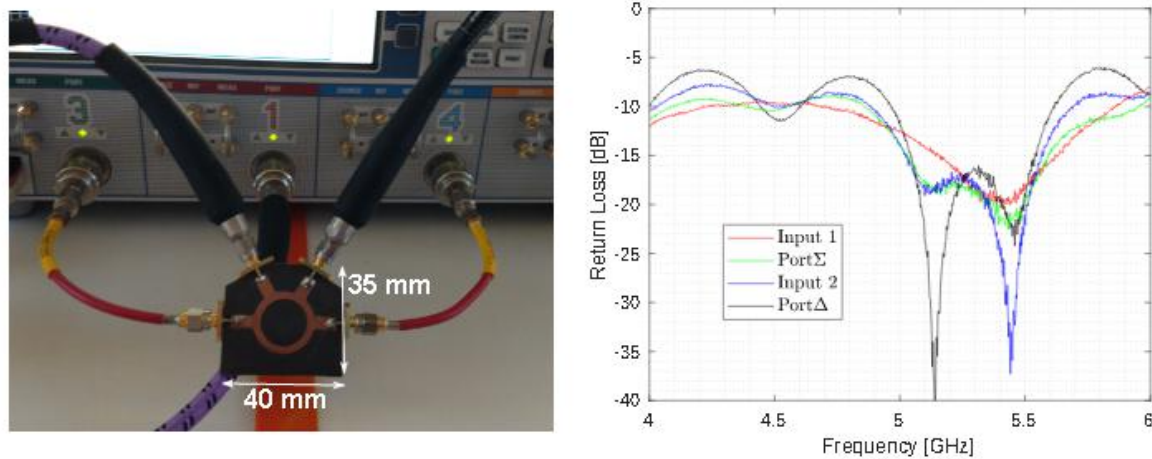
Fig. 5. Left, fabricated 180° planar hybrid and the measured return loss for its four ports (right).
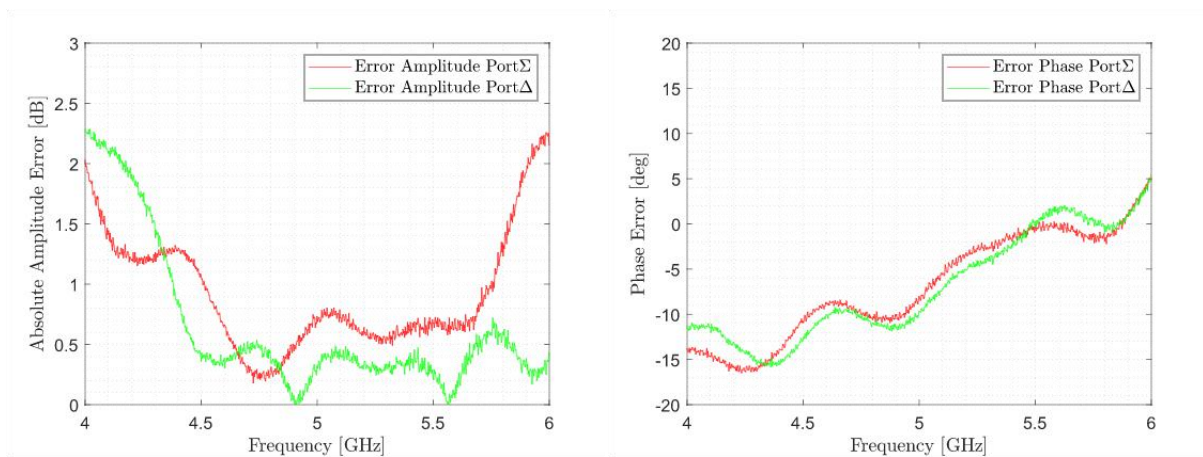

Fig. 6. Absolute amplitude (left) and phase (right) errors, measured at the Rat-race hybrid.

III.   FARFIELD PATTERN MEASUREMENTS

The array was set with both antennas spaced half-wavelength apart as to minimize side lobe level whilst keeping mutual coupling influences at bay. An RF switch was placed after the hybrid in order to electronically select the measured channel, with its 28 VDC control signal coming from a driver circuit. That enables the sequential monitoring of either sum and difference channels using a single spectrum analyzer. Fig. 7 shows the block diagram with the relay in detail. The P_{out} contains the received difference and sum ports power and is read out by a spectrum analyzer or network analyzer, the former providing an amplitude only information whereas the latter contains also the phase relations.
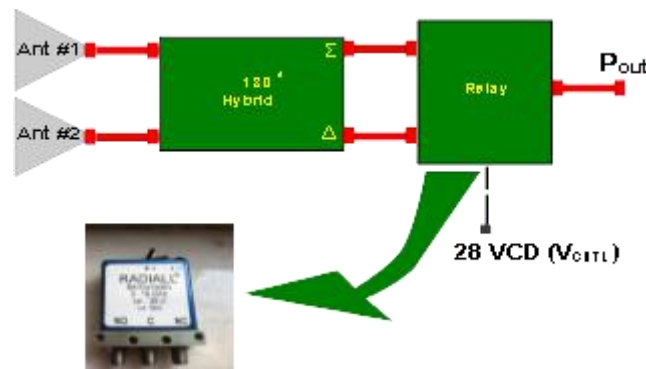
Fig. 7. Block diagram of the integrated monopulse, with the RF switch shown in detail.

The measurements were performed in the LME-USP chamber (Fig. 8), at the single frequency of 5.4 GHz, chosen within the joint operation band of both antennas and the rat-race hybrid. A patch antenna was used as replacement of the target in a real world tracking function, its dimensions similar to the ones used in the array, and was connected to a signal generator. The antenna array was kept inside the chamber with the beamformer network placed outside, minimizing stray electromagnetic couplings and structural reflections.
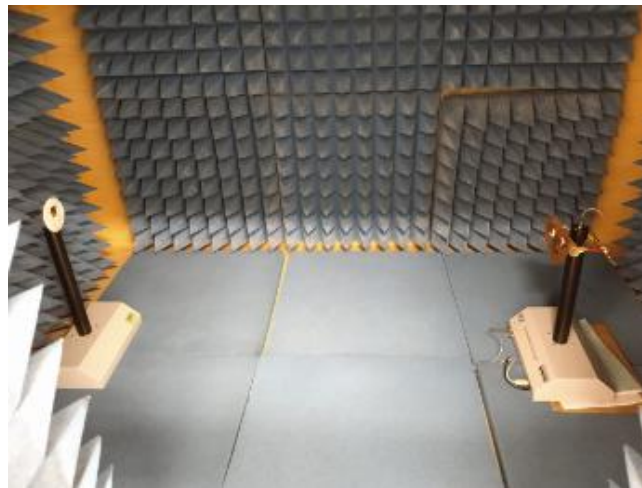

Fig. 8. Antenna array (right) positioned inside the LME-USP chamber.

The measured results are presented in Fig. 9. Simulations performed with FEKO are shown for the sake of comparison; the virtual model does not suffer from reflections and represents an ideal situation. It can be seen a small angle offset in the measurement, result of a misalignment inside the chamber. Effects of the wall reflections and support structure are seen on the energy contributions in angles larger than 90°. The two patch antennas were also not mechanically robust on their support

during the rotation, which explains the asymmetry on the lateral lobes, observed for either ports.
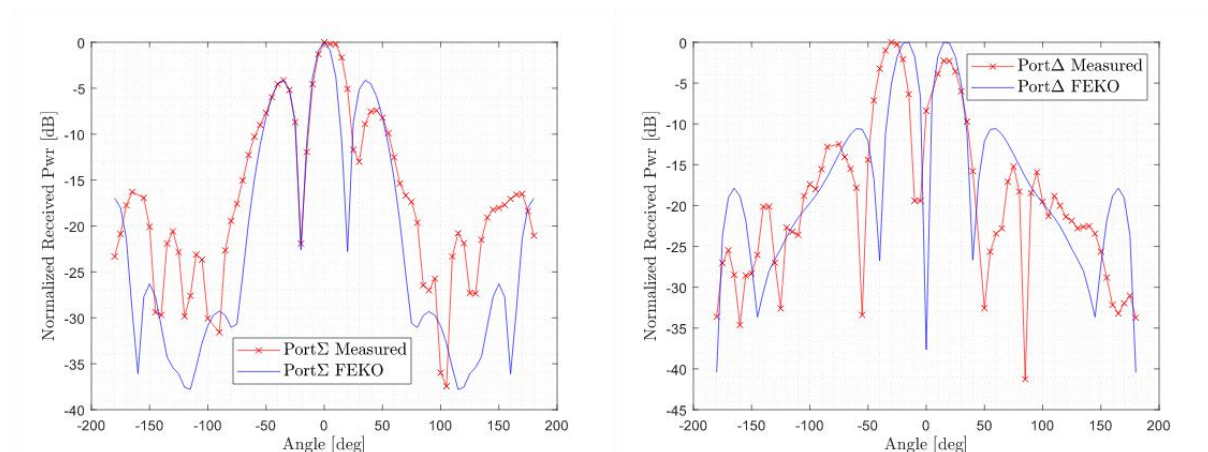

Fig. 9. Farfield patterns of the Sum/Σ (left), and Difference/Δ (right); measured and simulated.

Another set of measurements was performed in an un-shielded open indoor area, as to check its performance in case of its use in an ordinary laboratory for demonstration. Since the antenna rotation was done manually a smaller number of points was acquired in comparison to Fig. 8. From the results (Fig. 10), it can be seen that in spite of the far from ideal ambient the reflections from furniture, ceiling and floor do not differ from the ideal simulated farfield pattern responses. This scenario had the power pattern measured with a vector network analyzer (VNA) in place of the spectrum analyzer. In contrast to spectrum analyzers, VNAs offer some advantages in terms of dynamic range and phase information, but in general they suffer from lower output powers, which translates in smaller allowed distances between the transmitting and monopulse antennas. For this case, the distance between the antennas was set to 80 cm, equivalent to 14.4 λo at the measured frequency of 5.4 GHz.
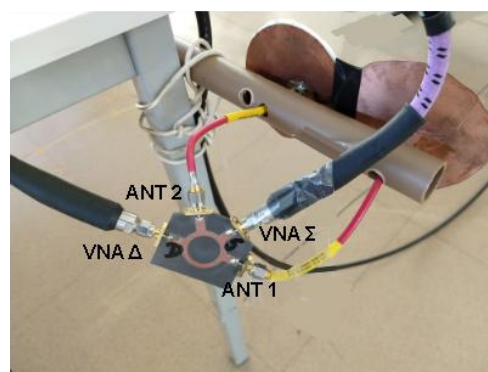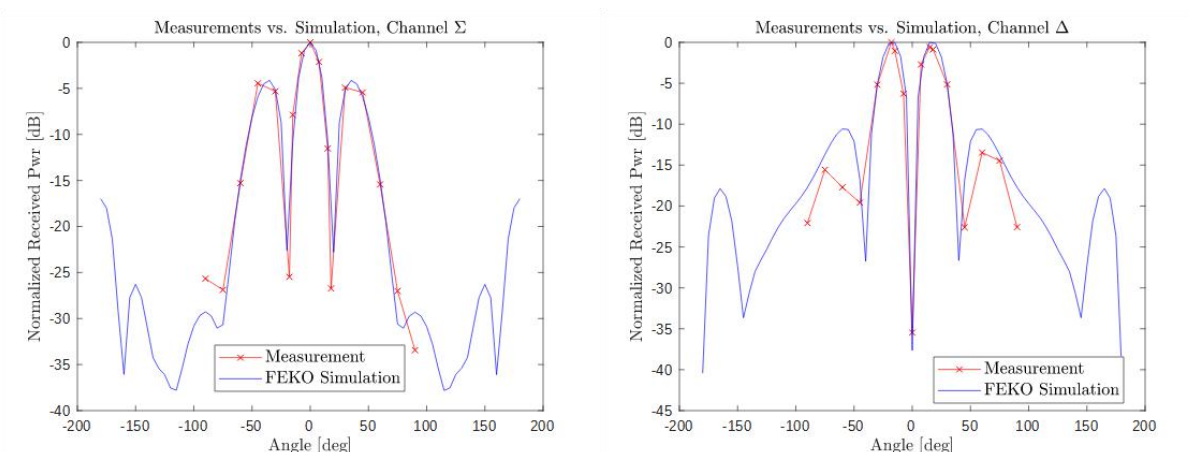
Fig. 10. Antennas in the mechanical PVC tubing support and connection to the hybrid (bottom) and farfield results (top left, sum port and bottom right, difference port).

IV. CONCLUSIONS

A low-cost C-Band monopulse radar is presented, with its design focusing on uncomplicated prototyping and styrofoam-dielectric patch antennas, with broad bandwidth and higher gain. Comparing to other C-band monopulses presented in the literature, this design has a simpler construction, with two single planar elements in place of the broadband 4x4 array deployed in a multi-layer (feed network and parasitic elements) [15]. The UWB monopulse presented in [16] is not purely planar, requiring a more complicated implementation. A monopulse based on a single patch, simultaneously excited in its TE10 and TE20 modes does not need a balun [17], though at expenses of a relatively narrow bandwidth and complex fabrication, based on a multilayer substrate-waveguide network. So the main contributions of this proposal are the styrofoam substrate that reduced the antenna quality thereby increasing the bandwidth and the RF relay connection, which allows the measurement with a single instrument, enabling a faster measurement system using, for instance, a software-defined radio.

Individual elements of the radar are shown with measurements and simulations, with good agreement. Final farfield measurements are shown in two different environments, also with

comparisons with ideal simulation scenarios. Results demonstrate the good performance in terms of expected field patterns even in indoor ambient.

REFERENCES

[1] J Genova, *Electronic Warfare Signal Processing*, ed. Artech House, Boston, 2018.

[2] [M. Skolnik, *Radar Handbook*, 3rd Edition, ed. McGraw Hill, 2008.

[3] B. R. Mahafza, *Radar Systems Analysis and Design Using Matla*b, 3rd Edition, ed. CRC Press, Boca Raton, 2013.

[4] K. S. Kwon, J. Park, W. Kim, H. S. Lee, D. Y Park, J. W. Heo, "Design X-band monopulse tracking system," *Microwave and Optical Technology Letters,* vol. 61, no. 8, pp. 2207-2032, Aug. 2019.

[5] H. Z. Zhang, C. Granet, M.A. Sprey, "A compact Ku-Band Monopulse Horn," *Microwave and Optical Technology Letters*, vol. 34, no. 1, pp. 9-13, Jul. 2002.

[6] P. Zheng, G. Q. Zhao, S. H. Xu, F. Yang, H. J. Sun, "Design of a W-Band Full-Polarization Monopulse Cassegrain Antenna," *IEEE Antennas and Wireless Propagation Letters*, vol. 16, pp. 99-103, 2017.

[7] J. L. Masa-Campos, S. Sanchez-Sevilleja, C. Dominguez-Grano-De-Oro, M. Sierra-Perez, J. L. Fernandez-Jambrina, "Monopulse beam-scanning planar array antenna in L-band," *Microwave and Optical Technology Letters*, vol. 50, no. 7, pp. 1812-1819, Jul. 2008.

[8] L. Yan, W. Hong, K. Wu, "Simulation and experiment on substrate integrated monopulse antenna," *2005 IEEE Antennas and Propagation Society International Symposium*, Jul. 2005, pp. 528-531.

[9] M. Poveda-Garcia, J. A. Lopez-Pastor, A. Gomez-Alcaraz, L. M. Martinez-Tamargo, M. Perez-Buitrago, A. Martinez-Sala, D. Canete-Rebenaque, J. L. Gomez-Tornero, "Amplitude-Monopulse Radar Lab using WiFi cards," *2018 48th European Microwave Conference (EuMC)*,2018, pp. 464-467.

[10] [D. Bonefacic, J. Jancula, "Laboratory Model of a Monopulse Radar Tracking System," *Proceedings of 48th International Symposium ELMAR,* 2006, pp. 227-230.

[11] R. Poisl, *Principles of Electronic Warfare Antenna System*s, ed. Artech House, Boston, 2011.

[12] B. Liu, W. Chang, X. Liu, "Design and Implementation of a monopulse radar signal processor," *Proceedings of the 19th International Conference Mixed Design of Integrated Circuits and Systems - MIXDES,* 2012, pp. 484-488.

[13] Y. X. Zhang, Q. F. Liu, R. J. Hong, P. P. Pan, Z. M. Deng, "A Novel Monopulse Angle Estimation Method for Wideband LFM Radars," *Sensors*, vol. 16, no. 6, pp. 817-830, 2016.

[14] Z. N. Chen, M. Y. W. Chia, *Broadband Planar Antennas: Design and Applications*, ed. Wiley, West Sussex, 2006.

[15] Z. W. Yu, G. M. Wang, C. X. Zhang, "A Broadband Planar Monopulse Antenna Array of C-Band," *IEEE Antennas and Wireless Propagation Letters*, vol. 8, pp. 1325-1328, Dec. 2009.

[16] N. Razazadeh, L. Shafai, "Ultrawideband monopulse antenna with application as reflector feed," *IET Microwaves, Antennas & Propagation*, vol. 10, no. 4, pp. 393-400, 2016.

[17] S. Youn, T. H. Lim, B. J. Jang, H. Choo, "Design of a Monopulse System Using a Single Patch Radiator with a Simple Multi-Mode Substrate Integrated Waveguide Feeding Network," *Applied Sciences*, vol. 10, no. 20, pp. 7224, 2020.